

Analytical and Experimental Study of Pile Capacity in Unsaturated Sandy Clay

H. Pujiastuti¹, A. Rifa'i², A.D. Adi², T.F. Fathani^{2,3}

Abstract – The design of pile foundation in technical practice is based on saturated soil mechanic or empirical procedure that ignores the influence of matric suction. Understanding the pile behavior and predicting the capacity of pile in unsaturated soil are important topics in foundation design. An experimental model test has been conducted on a single concrete pile model with a diameter of 16 mm and L/d ratios of 6, 10, 15 and 20. Model pile has been driven into sandy clay in the test box and is subjected to compression and uplift loading. The tensiometer instrument has been used to measure matric suction and the SoilVision has been used to get an estimate of the entire Soil Water Characteristic Curve (SWCC). The shear strength of sandy clay has been examined using a series of unconsolidated undrained triaxial tests to identify the relationship between cohesion, internal friction angle, and matric suction. The result has shown that end bearing pile capacity, skin friction capacity and total capacity of single piles are significantly influenced by the contribution of matric suction. Based on the experimental result, end bearing capacity and skin friction capacity of pile in saturated soil equation have been modified to calculate total capacity of pile in unsaturated soils by considering the influence of matric suction.

Keywords: Pile foundation, matric suction, modified analytical formula, SWCC, tensiometer

Nomenclature

| | | | |
|----------------------|---|----------------------|--|
| A_b | Cross sectional area | $Q_{b-unsat}$ | Ultimate end bearing capacity of the Pile in unsaturated soils |
| A_s | Area of shaft in contact with the soil | Q_s | Ultimate skin friction capacity of the pile |
| α | Adhesion factor | $Q_{s-unsat}$ | Ultimate skin friction capacity of the pile in unsaturated soils |
| α_{cr} | Corrected adhesion factor. | Q_t | Ultimate total pile capacity |
| c_u | Undrained cohesion | Sr | Residual suction value |
| $c_{u-unsat}$ | Undrained cohesion of unsaturated soils. | s_c, s_q, s_γ | Shape factor |
| $c_{ub-unsat}$ | Undrained cohesion of unsaturated soils at the base of the pile | $(u_a - u_w)$ | Matric suction |
| D | Diameter ratio of the soil media | w | Initial water content |
| D_{50} | 50 percent of the total grain weight is smaller than a certain grain size | | |
| d | Pile diameter | | |
| d_c, d_q, d_γ | Depth factor | | |
| d_{c-cr} | Corrected depth factor | | |
| δ | Angle of interface along the pile and soil | | |
| ϕ | Internal friction angle | | |
| γ | Unit weight of soil | | |
| i_c, i_q, i_γ | Load inclination factor | | |
| K_s | Coefficient of horizontal soil stress which depends on soil condition | | |
| L | Pile length | | |
| N_c, N_q, N_γ | Bearing capacity factor | | |
| $\frac{P'_b}{P_0}$ | Effective vertical pressure at pile base | | |
| P_0 | Average effective overburden pressure at pile base | | |
| Q_b | Ultimate end bearing capacity | | |

I. Introduction

The pile foundation is a slender structural element, which is located underneath the upperstructures [1]-[24].

Generally, it is used to support the building and to transfer the upperstructural load into the hard soil that is very deep [1]. It is also used when the soil beneath the surface is very shallow [2]. The method of pile installation, dissipation of excess pore pressures generated during installation, pile loading, stiffness and shear strength characteristics of the surrounding soil, and the soil-pile interface all have an impact on the bearing capacity of pile foundations [3]. Longer piles utilization on the nailed-slab system increases its bearing capacity [4]. The behavior of pile capacity is usually studied using experimental and numerical studies based on saturated soil mechanics principles, which assumes the weakest

natural soil is found under unsaturated conditions due to the very deep ground water table. The mechanical behavior of unsaturated soils is very different from saturated ones. The changes in matric suction do not have the same effect as the ones due to applied stresses, and consequently the effective stress principle is not applicable [5]. Several experimental and semi-empirical methods have revealed that matric suction has a considerable impact on shear strength [6]-[8]. The results of the research carried out by [8] have stated that the shear strength depends on matric suction in unsaturated sandy clay. The shear strength parameters are important in calculating the pile foundation capacity in unsaturated sandy clay [9]. Several studies have been conducted to investigate the effect of matric suction on the behavior of pile foundations in unsaturated soils based on both experimental and numerical modelling studies [10]-[15]. Furthermore, the analytical methods using several theories and validated by the field load test have been conducted by [16]. The influence of matric suction on the behavior of pile foundations in unsaturated sandy clay using analytical method has been also conducted by [9].

The end bearing, the skin friction, and the total pile capacity have increased nonlinearly with the increasing of matric suction. The physical behavior of the pile driven into sandy clay shows that on low matric suction, the value of the skin friction pile capacity tends to be higher than the one of the end bearing pile capacity. At a certain matric suction value, the skin friction pile capacity tends to be flat while the value of the end bearing pile capacity tends to increase. Due to the low value of the skin friction capacity on the short piles, the value of the end bearing capacity exceeds the value of the skin friction. It does not occur at the long pile because the value of skin friction capacity increases. In order to investigate the validity of the modified- α , β , and λ methods used by [17], a series of model pile load experiments were undertaken in a laboratory on statically compacted fine grained soil (i.e. compacted Indian Head till). The test findings reveal that the modified-, and approach gave a reasonable match to the model pile load test results performed in a laboratory. This paper is to propose the equation of modified skin friction capacity and the equation of modified end bearing capacity in order to estimate the total capacity of the pile in unsaturated soil. The required parameters in the equation of the pile friction capacity and end bearing capacity are determined by laboratory tests. A tensiometer is used to measure the matric suction in order to determine the soil water characteristic curve (SWCC).

A set of unconsolidated undrained triaxial experiments are used to investigate the shear strength parameters of unsaturated sandy clay. In order to get unsaturated undrained cohesion parameters and the internal friction angle, the connection with a matric suction supported by Soil Water Characteristic Curve (SWCC) is needed. The relationship is expressed in the matric suction function. It can be used to estimate the value of cohesion and the internal friction angle in the matric suction variation. A

series of pile load tests have been carried out on a statically compacted sandy clay soil with varying water content to study the validity of the proposed modification equation. The corrected adhesion factor for unsaturated sandy clay is determined by the back calculation of the friction pile capacity equation with the test result of the pile model subjected to uplift loads. The corrected depth factor for unsaturated sandy clay is determined by back calculation of the end bearing capacity equation with the test results of the pile models subjected to compressive load deducted by the test result of the pile models subjected to uplift loads.

II. Calculating Ultimate Pile Capacity in Saturated-unsaturated Sandy Clay

This section provides the procedures in calculating the ultimate pile capacity in saturated and partially saturated soils. The ultimate total pile capacity in saturated soil is calculated from the sum of the ultimate end bearing and the ultimate skin friction capacity. Pile in soils intermediate between sand and clay, alternatively the base resistance, can be calculated from the equation of shallow foundation bearing capacity [18]. For the soils having both the undrained cohesion and the internal friction angle, i.e. sandy clay, the ultimate end bearing capacity of the circular shape foundation in saturated soil is calculated with Meyerhof's general equation, expressed in Eq. (1).

$$Q_b = A_b(c_u N_c s_c d_c i_i + P'_b N_q s_q d_q i_q + 0.5 \gamma d N_\gamma s_\gamma d_\gamma i_\gamma) \quad (1)$$

where Q_b is the ultimate end bearing capacity, A_b is the cross sectional area, P'_b is the effective vertical pressure at pile base, N_c, N_q, N_γ is the bearing capacity factor, γ is the unit weight of soil, d is the pile diameter, s_c, s_q, s_γ is the shape factor, d_c, d_q, d_γ is the depth factor, and i_c, i_q, i_γ is the load inclination factor. The ultimate skin friction capacity of the pile considers the contribution of undrained cohesion and internal friction angle as expressed in Eq. (2).

$$Q_s = (\alpha c_u A_s) + (K_s \bar{p}_0 \tan \delta A_s) \quad (2)$$

where Q_s is the ultimate skin friction capacity of the pile, α is the adhesion factor, c_u is the undrained cohesion, A_s is the area of shaft in contact with the soil, K_s is a coefficient of horizontal soil stress which depends on soil condition, \bar{p}_0 is the average effective overburden pressure at pile base, δ is angle of interface along the pile and soil. Researchers in [9] have proposed the formula in Eq. (3) and Eq. (4) in order to calculate the ultimate end bearing and skin friction capacity, respectively in unsaturated soil. The unsaturated parameters involved in the formula in Eq. (3) and Eq. (4) have been obtained from the results of the laboratory

testing. The ultimate end bearing of the circular shape foundation is expressed in Eq. (3).

$$Q_{b-unsat} = A_b(c_{ub-unsat} N_c s_c d_c i_c + P_b N_q s_q d_q i_q + 0.5 \gamma d N_{\gamma} s_{\gamma} d_{\gamma} i_{\gamma}) \quad (3)$$

where $Q_{b-unsat}$ is the ultimate end bearing capacity of the pile in unsaturated soils, $c_{ub-unsat}$ is the undrained cohesion of unsaturated soils at the base of the pile. The ultimate skin friction capacity of the circular shape foundation is expressed in Eq. (4).

$$Q_{s-unsat} = (\alpha c_{u-unsat} A_s) + (K_s \bar{p}_0 \tan \delta A_s) \quad (4)$$

where $Q_{s-unsat}$ is the ultimate skin friction capacity of the pile in unsaturated soils, $c_{u-unsat}$ is the undrained cohesion of unsaturated soils.

III. Materials, Testing Methodology and Equipment Set Up

Under static loading circumstances, a set of model pile load tests have been conducted in saturated and partially saturated compacted sandy clay. The purpose of the experimental testing is to see how matric suction affects the ultimate pile capacity of various pile models.

III.1. Soil Properties

The soil sample used in the study is made up of 40% clay and 60% sand from Yogyakarta's Piyungan Subdistrict and Depok Subdistrict.

The soil samples have been tested for their index properties. The results of the index properties test are shown in Table I. It has been proposed to determine the ultimate pile capacity of model piles at three different water contents i.e., 23 % (optimum), 17 % (dry optimum) and 28.05 % (saturated). These water contents have been chosen from standard Proctor test. The specimens were statically compacted to reach the same dry density (15.1 kN/m³) despite having three varying water contents. Using a tensiometer, the matric suction values of the tested compacted soils in the test box were directly determined [15]. The measured matric suction values have been 73.67 kPa, 53.61 kPa and 0 kPa for water contents of 17 %, 23 % and 28.05 %, respectively.

The specimens prepared at nine different water contents were compacted statically in the nine CBR moulds to attain the same dry density (15.1 kN/m³) in order to determine the soil water characteristic curve (SWCC). The link between the degree of saturation and matric suction was plotted using the results of tensiometer measurements of specimens. Using an appropriate curve fitting equation that represents measurable data points, the SoilVision has been used to approximate the full SWCC. In this research, Fredlund and Xing's equation presented in Fig. 1 has been used.

The air entry values (AEV) and the residual suction value (S_r) of sandy clay have been 28.06 kPa and 210 kPa, respectively.

III.2. Testing Methodology and Equipment Set up

The test box has been constructed with internal dimensions of 110 cm × 110 cm × 110 cm. The materials used for constructing the box have consisted of a series of 9.5 mm thick steel plate and 40 mm × 60 mm × 5 mm thick hollow steel section (HSS) as the frame and stiffeners. The materials used for the construction of the box have been rigid enough to function as an independent reaction frame. The vertical stress in the soil may decrease due to friction between the soil and the wall of the test box. In order to minimize such interference, the inside walls of the soil bin have been polished smooth in order to reduce friction with soil as much as possible. This research applies the diameter ratio of the soil media (D) against the one of the model (d) greater than eight or $D/d > 8$, in order to avoid the influence of soil media boundaries. Moreover, the pile diameter greater than $20 \times D_{50}$ (grain size) has been used in order to avoid the influence of scale effect. The model pile is too close to the boundary of the test box, affecting the stress and the displacement of the soil. Therefore, the zone of influence is in the range of 3-8 times the pile diameter. The distance between the boundaries of the box to the pile model in the horizontal direction is 12 times the diameter of the pile, while the vertical direction is 8 times the diameter of the pile [19].

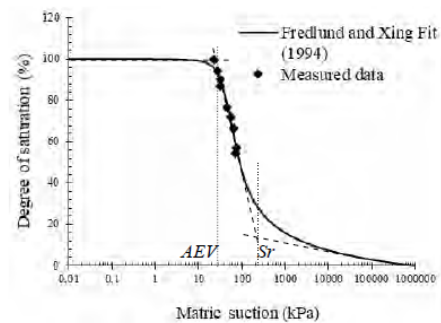


Fig. 1. The measured SWCC of sandy soil based on tensiometer

TABLE I
PROPERTIES OF THE TESTED SOIL

| Soil Properties | Value |
|----------------------------------|-------|
| Specific Gravity, G _s | 2.66 |
| Liquid Limits, LL (%) | 36.79 |
| Plastic Limits, PL (%) | 21.36 |
| Plasticity Index (%) | 15.43 |
| Soil fraction: | |
| Clay (%) | 9.73 |
| Silt (%) | 51.66 |
| Sand (%) | 38.61 |

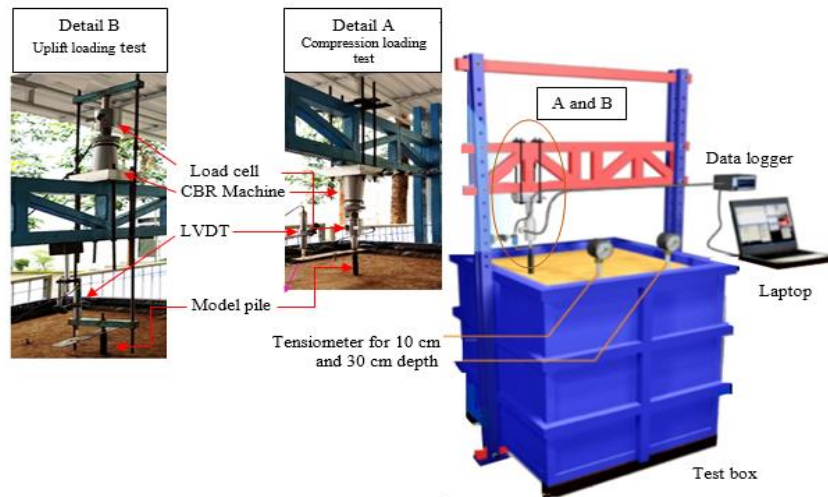


Fig. 2. Test set up for model pile compression loading test (Detail A) and uplift loading test (Detail B)[20]

The field soil sample has been air-dried for several days, pulverized, and passed through a sieve with a 2 mm aperture size (i.e. #10 sieve). The soil sample has been combined with water at a set beginning initial water content. To guarantee equal water content conditions throughout the sample, the prepared soil water combination was placed in sealed plastic bags and then stored for one day. It should be noted that the sandy clay-water mixture (hereafter referred to as soil) has been prepared in ten layers placed at about 100 mm thick in box. Soil was deposited in the test box and compacted with a 10.96 kg compactor in 100 mm thick layers. All of the layers in the test box were compacted in the same way. After the soil has been compacted per layer, the core cutter test has been done in order to determine the density of soil (it is appropriate with maximum dry density of standard compaction test result). The average dry density of the soil in the box is 95 % of the optimum dry density. The model pile used in the study has been made out of circular concrete with 16 mm diameter (d). The pile length (L) have been 96 mm, 160 mm, 240 mm and 320 mm, which correspond to (L/d) ratios of 6, 10, 15 and 20, respectively. Model piles have been driven into the depths of 96 mm, 160 mm, 240 mm and 320 mm. The pile have been tested in axial compression and uplift load, the test set up shown in Fig 2. The compression and uplift load has been applied with constant rate of penetration method. A pile penetration rate of 0.85 mm/minute referred to ASTM D1143-81 for the compression load and ASTM 3689-9 for the uplift load. The applied load and the displacement of the pile have been recorded during the compression/uplift load test. The linear variable displacement transducer (LVDT) has been installed at the pile head in order to measure the pile displacement. In this research, the 30-WF6209 LVDT with a stroke length of 50 mm has been used. This model has been supplied with a spring loaded shaft, subjected to the fully extended position. The accuracy of

LVDT readings is 0.01 mm. The 28-WF6453 load cell has been used to measure the applied compression/uplift load at the pile head. The accuracy of the load cell readings is 0.01 kg. LVDT and the load cells are connected with a 30-WF6016 Geodatalog series 6000 data logger to collect and record data and has been processed by a laptop computer. The tensiometers used for the test program have an operating range from 0 to 100 kPa in order to measure matric suction. More details related to experimental test equipment have been reported by Pujiastuti [20].

IV. Result and Discussion

IV.1. Undrained Cohesion and Internal Friction Angle

The undrained cohesion (c_u) and the internal friction angle (ϕ) in unsaturated sandy clay are obtained by modified Unconsolidated Undrained (UU) Triaxial Test conducted by [8]. Matric suction values used in the calculations are obtained from the tensiometer readings for the related depths. The corresponding matric suction value for the related degree of saturation value has been estimated from the soil water characteristic curve (SWCC). Based on Fig. 3, the undrained cohesion (c_u) expressed as a function of the matric suction ($u_a - u_w$) is determined by Eq. (5).

$$c_u = -0.0044(u_a - u_w)^2 + 0.9486(u_a - u_w) + 20.223 \quad (5)$$

While internal friction angle (ϕ) expressed as a function of the matric suction ($u_a - u_w$) is determined by Eq. (6) and showed in Fig. 4.

$$\phi = -0.0027(u_a - u_w)^2 + 0.5705(u_a - u_w) + 1.7788 \quad (6)$$

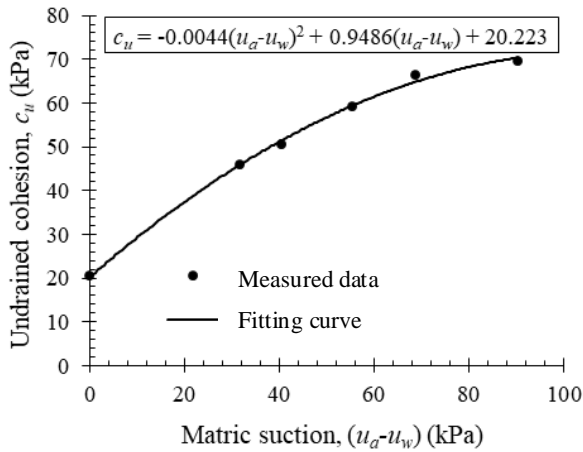


Fig. 3. The relationship between undrained cohesion and matric suction based on laboratory test

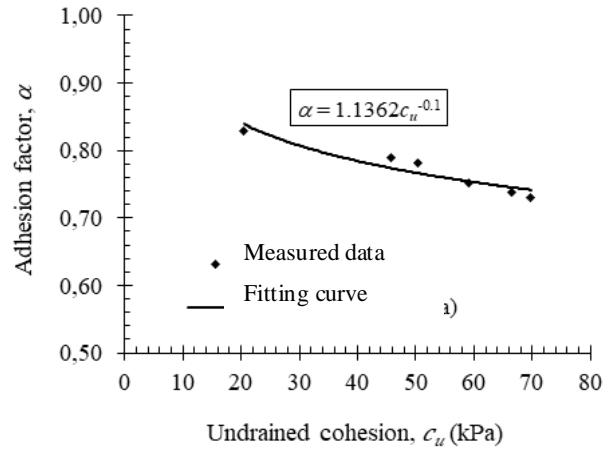


Fig. 5. The relationship between adhesion factor and undrained cohesion based on laboratory test

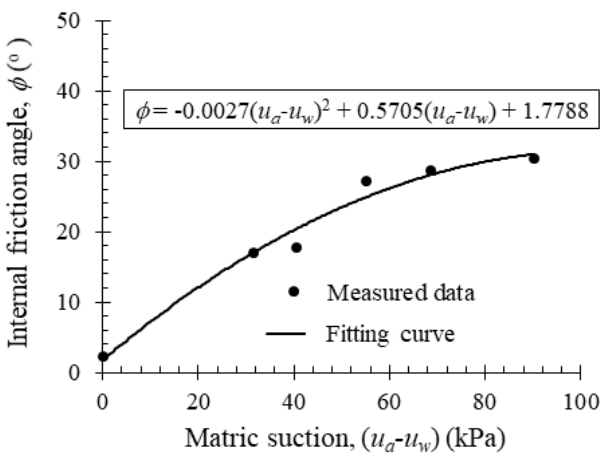


Fig. 4. The relationship between internal friction angle and matric suction based on laboratory test

IV.2. Adhesion Factor (α)

In this study, the adhesion factor (α) has been determined from the laboratory test results, by dividing the adhesion of concrete and soil material (c_d) obtained from the direct shear test with undrained cohesion (c_u) obtained by the modified UU Triaxial Test conducted by [8] as expressed in Eq. (7).

$$\alpha = \frac{c_d}{c_u} \quad (7)$$

The relationship between the adhesion factor (α) undrained cohesion (c_u) is shown in Fig. 5. The adhesion factor (α) expressed as a function of undrained cohesion (c_u) is determined by Eq. (8).

$$\alpha = 1.1362c_u^{-0.1} \quad (8)$$

The adhesion factor (α) decreases with increasing undrained shear strength (c_u) of the soil. This is in line with the results of studies conducted by [21].

IV.3. Model Pile Test Result

Figure 6 shows the results of model piling tests conducted in both saturated and partially saturated soil conditions. Model pile is driven into the compacted soil with different compaction water contents (i.e., 28.05 %, 23 %, and 17 %). The end bearing, the skin friction and total pile capacity are vary greatly depending on the soil conditions i.e saturated and unsaturated and the length of pile with L/d ratio varies 20, 15, 10 and 6 while d is 16 mm. The ultimate skin friction capacity has been determined by using the data of uplift load test results, the ultimate total pile capacity has been determined by using the data of compressive load test results, and the ultimate end bearing capacity has been calculated by subtracting the ultimate skin friction capacity and the ultimate total pile capacity. Based on the ultimate capacity of the model pile test results (Fig. 6), it is clarified that the ultimate end bearing, the ultimate skin friction, and the ultimate total pile capacity have increased nonlinearly with the increase of the matric suction. This is because the increased matric suction increases the shear strength. The inter-particle force produced by the negative pore water pressure is linked to higher soil shear strength [8]. In the other words, the shear strength has controlled the pile foundation capacity in unsaturated soils. This is in agreement with the results of the study conducted by [10]. The physical behaviours of the long pile ($L/d=20$ and $L/d=15$) are presented in Fig. 6a and 6b. The total pile capacity has increased significantly in all the observed matric suctions. The total pile capacity has the highest capacity value, followed by skin friction and end bearing capacity. At a certain value of the matric suction, the skin friction value tends to be flat while the end bearing value rises more significantly. The physical behaviours of the short piles ($L/d=6$ and $L/d=10$) is presented in Fig. 6c and 6d. At low matric suction to the certain value of matric suction, end bearing, skin friction, and total pile capacity increase slowly. After exceeding the certain value of the matric

suction, the total pile capacity and the end bearing friction has tended to be flat.

The physical behaviour of the long and the short piles is agreement with the results of study conducted by [9].

The percentage of the ultimate skin friction capacity (Q_s) and the ultimate end bearing capacity (Q_b) components in the ultimate total pile capacity (Q_t) is calculated by using (9) and (10).

$$\text{Load sharing } Q_s \text{ on } Q_t = \frac{Q_s}{Q_t} \times 100\% \quad (9)$$

$$\text{Load sharing } Q_b \text{ on } Q_t = \frac{Q_b}{Q_t} \times 100\% \quad (10)$$

The results of the load sharing calculations Q_s and Q_b are shown in Table II. In saturated soil conditions (zero matric suction), the load distribution mobilized from the collapsed pile has been dominated by the skin friction pile. This is agreement with the results of study conducted by [9]. The average load distribution of the skin friction pile has been 86.13 % and 74.29 % of the total pile capacity for long and short pile, respectively. The domination of the skin friction pile is associated with

capacity have increased rather significantly, but skin the saturated soil in soft and not dense condition. At matric suction of 53.61 kPa (i.e. in unsaturated soil condition), the load distribution mobilized from the collapsed pile has been dominated by the skin friction pile for long pile. The average load distribution of the skin friction pile has been 57.19 % of the total pile capacity. For short pile, the collapsed pile has been dominated by the end bearing pile. The average load distribution of the end bearing pile has been 59.55 % of the total pile capacity. The domination of end bearing pile is related to small pile shaft area at short pile. It has lead to the skin friction pile capacity relatively low.

Furthermore, at matric suction of 73.67 kPa (i.e. in unsaturated soil condition), the load distribution mobilized from the collapsed pile has been dominated by the end bearing pile. The average load distribution of the end bearing pile has been 53.43 % and 71.82 % of the total pile capacity for long and short pile, respectively. The domination of the end bearing piles is related to stiff dense soil conditions at high matric suction. In such conditions, the increase in end bearing pile is more significant than skin friction pile.

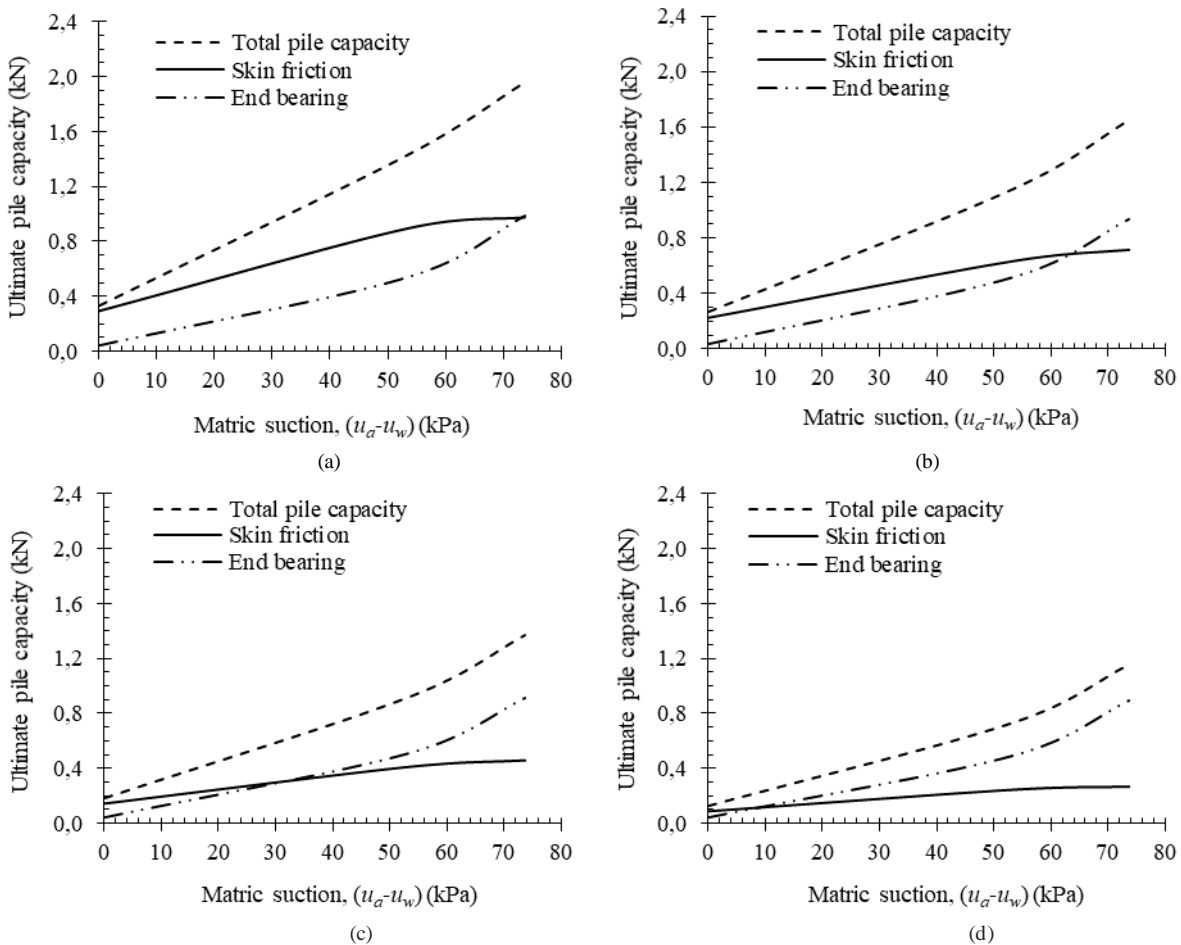


Fig. 6. Ultimate pile capacity with variation of matric suction by different L/d ratios: (a) 20; (b) 15; (c) 10 and (d) 6

TABLE II
LOAD SHARING BETWEEN THE SKIN FRICTION CAPACITY (Q_s) AND THE
END BEARING CAPACITY (Q_b) IN SANDY CLAY

| (u_a-u_w) | Load sharing Q_s on Q_t (%) | | | Load sharing Q_b on Q_t (%) | | |
|-------------|---------------------------------|-------|-------|---------------------------------|-------|-------|
| | 0 | 53.61 | 73.67 | 0 | 53.61 | 73.67 |
| Long pile | | | | | | |
| $L/d=20$ | 87.25 | 60.34 | 49.77 | 12.75 | 39.66 | 50.23 |
| $L/d=15$ | 85.01 | 54.05 | 43.37 | 14.99 | 45.95 | 56.63 |
| Average | 86.13 | 57.19 | 46.57 | 13.87 | 42.81 | 53.43 |
| Short pile | | | | | | |
| $L/d=10$ | 78.76 | 46.17 | 33.33 | 21.24 | 53.83 | 66.67 |
| $L/d=6$ | 69.82 | 34.74 | 23.03 | 30.18 | 65.26 | 76.97 |
| Average | 74.29 | 40.46 | 28.18 | 25.71 | 59.54 | 71.82 |

IV.4. Pile Capacity Calculation

The model pile capacity test results have been calculated using the equation of the end bearing and the skin friction capacity, while the total pile capacity has been calculated by adding up the value of the end bearing and skin friction capacity. The pile model with L/d ratio varies 20, 15, 10, 6 and d is 16 mm and it has been tested in compacted soil sample prepared with different initial water contents (i.e. 28.05 %, 23 % and 17 %).

The end bearing of the tested pile has been calculated by using Eq. (3). The bearing capacity factor, N_c, N_q, N_γ , the shape factor, s_c, s_q, s_γ , the depth factor, d_c, d_q, d_γ and the load inclination factor, i_c, i_q, i_γ are determined by using Meyerhof's equation. In this study, the load position is vertical so the value of the load inclination factor i_c, i_q, i_γ is assumed to be 1.

Table III shows the measurement and the calculation of the ultimate end bearing pile capacity test results. The skin frictions of tested pile have been calculated by using Eq. (4).

A value of c_u is calculated by using Eq. (5), α is calculated by using Eq. (8). K_s value is assumed to be equal to 1 for saturated condition and 5 for unsaturated condition. For saturated condition, $K_s \tan \delta$ value is much lower as it reflects the effect of looser soil conditions (low soil clamping) near the shaft pile after the collapse of soil into the cavity below the pile tip.

TABLE III
COMPARISON BETWEEN THE MEASUREMENT AND CALCULATION OF
ULTIMATE END BEARING CAPACITY USING EQ. (3)

| $c_u^{(1)}$ kPa | $w^{(2)}$ % | (u_a-u_w) kPa | L/d | $d_c^{(3)}$ | $d_{c-cr}^{(4)}$ | Calc $Q_b^{(5)}$ kN | Meas. Q_b kN |
|--------------------|----------------|--------------------|-------|-------------|------------------|------------------------|-------------------|
| 20.22 | 28.05 | 0 | 20 | | 1.53 | 0.04 | 0.04 |
| | | | 15 | 1.21 | 1.43 | 0.04 | 0.04 |
| | | | 10 | 1.40 | 0.04 | 0.04 | |
| | | | 6 | 1.36 | 0.04 | 0.04 | |
| 58.43 | 23 | 53.61 | 20 | | 1.71 | 0.59 | 0.59 |
| | | | 15 | 1.31 | 1.58 | 0.54 | 0.54 |
| | | | 10 | 1.41 | 0.48 | 0.48 | |
| | | | 6 | 1.36 | 0.46 | 0.46 | |
| 66.22 | 17 | 73.67 | 20 | | 1.64 | 0.98 | 0.98 |
| | | | 15 | 1.34 | 1.57 | 0.93 | 0.93 |
| | | | 10 | 1.55 | 0.92 | 0.92 | |
| | | | 6 | 1.51 | 0.89 | 0.89 | |

(u_a-u_w) : matric suction

⁽¹⁾Undrained cohesion calculated by using Eq. (5)

⁽²⁾Initial water content

⁽³⁾Depth factor calculated by using Meyerhof's equation

⁽⁴⁾Recalculated of depth factor obtained using Eq. (11)

⁽⁵⁾Calculated end bearing capacity by using Eq. (3) and d_{c-cr} value

The angle of the friction between the pile surface and the soil (δ) and the effective angle of shearing resistance (ϕ) over the length of the pile shaft has been assumed to be the same as for the precast concrete pile [18]. In this study, ϕ is a function of matric suction and it is determined by using Eq. (6). Matric suction values used in the calculations are obtained from the tensiometer readings. Table IV shows the measurement and the calculation of ultimate skin friction pile capacity test results.

Both the values of the measurement and the calculation results are the same due to the contribution of matric suction. It can be concluded that the difference between the measurements and the calculation of the value of the end bearing capacity can be related to the depth factor (d_c) that depend on the stress conditions, while the difference between the measurements and the calculation of the value of pile friction capacity can be related to the value of the adhesion factor (α). For this reason, the value of depth factor (d_c) and the adhesion factor (α) have been recalculated to understand the effects of unsaturated soil conditions.

The depth factors have been recalculated from the pile model test results as expressed in equation Eq. (11).

$$d_{c-cr} = \frac{\frac{Q_b}{A_b} - (P_b' N_q s_q d_q) - (0.5 \gamma d N_\gamma s_\gamma d_\gamma)}{c_{u-unsat} N_c s_c} \quad (11)$$

where d_{c-cr} is the corrected depth factor. The results of the corrected depth factor (d_{c-cr}) is summarized in Table III.

The proposed depth factor for end bearing equation modification as a function of undrained cohesion has been expressed in Eq. (12) and presented in Fig. 7.

$$d_{c-cr} = 1.1102 c_u^{0.0792} \quad (12)$$

The adhesion factor (α) has been determined for saturated and unsaturated condition based on laboratory test result as discussed in earlier sections. The adhesion factor (α) has been recalculated from the pile model test results.

TABLE IV
COMPARISON BETWEEN THE MEASUREMENT AND CALCULATION OF
ULTIMATE SKIN FRICTION CAPACITY USING EQ. (4)

| c_u kPa | w % | (u_a-u_w) kPa | L/d | $\alpha^{(1)}$ | $\alpha_{cr}^{(2)}$ | Calc $Q_s^{(3)}$ kN | Meas. Q_s kN |
|--------------|----------|--------------------|-------|----------------|---------------------|------------------------|-------------------|
| 20.22 | 28.05 | 0 | 20 | | 0.90 | 0.29 | 0.29 |
| | | | 15 | 0.84 | 0.92 | 0.23 | 0.23 |
| | | | 10 | 0.88 | 0.14 | 0.14 | |
| | | | 6 | 0.89 | 0.09 | 0.09 | |
| 58.43 | 23 | 53.61 | 20 | | 0.84 | 0.90 | 0.90 |
| | | | 15 | 0.76 | 0.82 | 0.64 | 0.64 |
| | | | 10 | 0.82 | 0.41 | 0.41 | |
| | | | 6 | 0.83 | 0.24 | 0.24 | |
| 66.22 | 17 | 73.67 | 20 | | 0.80 | 0.98 | 0.98 |
| | | | 15 | 0.75 | 0.81 | 0.72 | 0.72 |
| | | | 10 | 0.80 | 0.46 | 0.46 | |
| | | | 6 | 0.80 | 0.27 | 0.27 | |

⁽¹⁾ α value calculated by using Eq. (8)

⁽²⁾Recalculated α value obtained using Eq. (13)

⁽³⁾Calculated skin friction capacity by using Eq. (4) and α_{cr} value

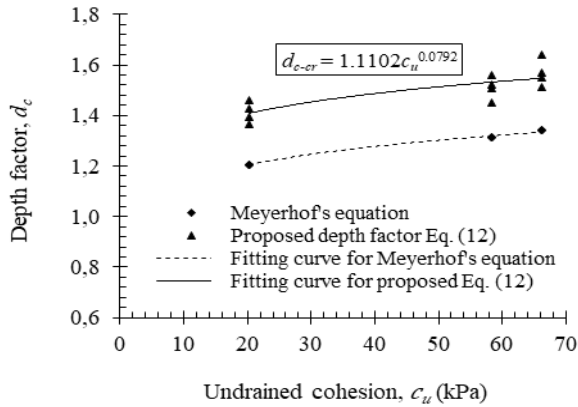


Fig. 7. The relationship between depth factor and undrained cohesion

The back calculation of the adhesion factor (α) has been determined by dividing the shear stress of the soil mobilized as a skin friction on the ultimate skin friction by the shear strength of the soil for each model test [22], as expressed in Eq. (13).

$$\alpha_{cr} = \frac{\frac{Q_s}{A_s} - K_s \bar{P}_0 \tan \delta}{c_{u-unsat}} \quad (13)$$

where α_{cr} is the corrected adhesion factor. The results of the corrected adhesion factor (α_{cr}) are summarized in Table IV. The proposed adhesion factor for skin friction equation modification as a function of undrained cohesion has been expressed in Eq. (14) and presented in Fig. 8.

$$\alpha_{cr} = 1.1847c_u^{-0.091} \quad (14)$$

Furthermore, the modified end bearing pile capacity equation ($Q_{b-unsat}$) and the modified skin friction pile capacity for pile foundations in unsaturated soils ($Q_{s-unsat}$) as expressed in Eq. (15) and Eq. (16) have been proposed.

$$Q_{b-unsat} = A_b(c_{u-unsat} N_c s_c d_{c-cr} i_i + P_b' N_q s_q d_q i_q + 0.5 \gamma d N_\gamma s_\gamma d_\gamma i_\gamma) \quad (15)$$

where $Q_{b-unsat}$ is the ultimate end bearing capacity of the pile in unsaturated soils, $c_{ub-unsat}$ is the undrained cohesion of unsaturated soils at the base of the pile and d_{c-cr} is the corrected depth factor. Both $c_{ub-unsat}$ and d_{c-cr} have been calculated by using Eq. (5) and Eq. (12).

$$Q_{s-unsat} = (\alpha_{cr} c_{u-unsat} A_s) + (K_s \bar{p}_0 \tan \delta A_s) \quad (16)$$

where $Q_{s-unsat}$ is the ultimate skin friction capacity of the pile in unsaturated soils, α_{cr} is the corrected adhesion factor, $c_{u-unsat}$ is the undrained cohesion. Both $c_{u-unsat}$ and α_{cr} have been calculated by using Eq. (5) and Eq. (14).

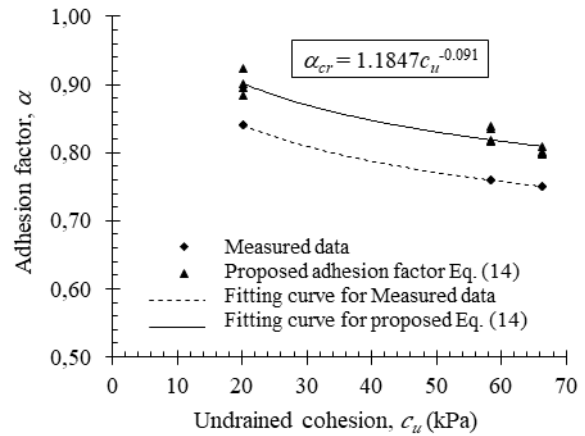


Fig. 8. The relationship between adhesion factor and undrained cohesion

V. Conclusion

The capacity of pile foundation (end bearing and skin friction pile capacity) that is driven into unsaturated sandy clay considers two parameters of soil shear strength i.e., undrained cohesion and internal friction angle of soil. Saturated soil parameters, which assume the weakest soil conditions, are commonly used for pile foundation design. In this study, the pile foundation capacity in unsaturated sandy clay has been calculated using the equation for modified saturated soil by involving matric suction using SWCC that has been adjusted using the SoilVision knowledge-based system.

A series of compression and uplift load tests on the model pile have been conducted on statically compacted sandy clay in a soil mechanical laboratory in order to study the effect of matric suction on the end bearing, the skin friction, the total pile capacity and to propose the modified equations from saturated equations.

The results show that the ultimate end bearing, the ultimate skin friction, and the ultimate total pile capacity increased with the increasing of matric suction. There is a tendency for a certain matric suction (i.e. 60 kPa) in which the skin friction value tends to be flat while the end bearing value rises more significantly. In saturated soil conditions, the ultimate total pile capacity is more dominated by the mobilization of the skin friction capacity than the end bearing capacity. The opposite conditions have experienced pile model in unsaturated soil at matric suction of 73.67 kPa, the ultimate total pile capacity is more dominated by the mobilization of the end bearing capacity. While the long pile model in unsaturated soil at matric suction of 53.61 kPa, the ultimate total pile capacity is dominated skin friction capacity and it is dominated end bearing capacity for short pile model. The modified equation for unsaturated soil and involvement of the undrained cohesion, the correction value of depth factor and adhesion factor have been validated with the model pile load test results under compression and uplift load conducted in soil mechanical laboratory.

Acknowledgements

The authors would like to express their gratitude to the Directorate General of Science and Technology Science and Higher Education Ministry of Research, Technology and Higher Education, Indonesia for the financial support through Education Scholarship Postgraduate Domestic Programs.

References

- [1] A. A. Jebur, W. Atherton, R.M. Alkhadar, and E. Loffill, Piles in Sandy Soil : A Numerical Study and Experimental Validation, *Creative Construction Conference, Procedia Engineering, Vol. 196, pp. 60 – 67, Primosten, Croatia, 19-22 June 2017.*
- [2] F. Z. Ait Quharouch, B. Bahrar, Kamal Gueraoui, Study of the Influence of the Soil and Pile Characteristics on the Behavior of a Pile Subjected to a Lateral Load, *International Review of Civil Engineering (IRECE), Vol 10 (No. 6): 320-325, 2019.*
- [3] M.F. Randolph, Science and Empiricism in Pile Foundation Design, *Géotechnique, Vol.53(No. 10):847–87, October 2003.*
- [4] A. Waruwu, H.C. Hardiyatmo, A. Rifa'i, The Performance of the Nailed Slab System-Supported Embankment on Peat Soil, *International Review of Civil Engineering (IRECE), Vol 10 (No. 5): 243-248, September 2019.*
- [5] M.Y. Fattah, K.R. Mahmood and M.M. Muhyee Al Dosary, Simulation of Unsaturated Soil Behavior by the Finite Element Method, *International Review of Civil Engineering (IRECE), Vol 4 (No. 1): 34-46, January 2013.*
- [6] C. Gallage and T. Uchimura, Direct Shear Testing on Unsaturated Silty Soils to Investigate the Effects of Drying and Wetting on Shear Strength Parameters at Low Suction, *J. Geotech. Geoenviron. Eng., ASCE, Vol. 142(No. 3):1-9, September 2015.*
- [7] A.M. Elsharief and O.A. Abdulaziz, Effects of Matric Suction on the Shear Strength of Highly Plastic Compacted, *The 16th African Regional Conference on Soil Mechanics and Geotechnical Engineering, pp.97-103, Tunis, April 2015.*
- [8] H. Pujiastuti, A. Rifa'i, A.D. Adi and T.F. Fathani, The Effect of Matric Suction on The Shear Strength of Unsaturated Sandy Clay, *International Journal of Geomate, Vol.14(Issue 42):112-119, Januari 2018a.*
- [9] H. Pujiastuti, A. Rifa'i, A.D. Adi and T.F. Fathani, Effect of Matric Suction Change on Pile Foundation Capacity in Unsaturated Soils, *International Conference on Geotechnics, Vol. 1, pp. 94-100, Yogyakarta, Indonesia, 24-26 July 2018b.*
- [10] O. Bandehzadeh, M.M. Sadeghi, M.A. Rowshanzami and A.H. Nia, Definition of the Load Carrying Capacity of Single Piles in Unsaturated Soils Using Barcelona Basic Constitutive Model, *Electronic Journal of Geotechnical Engineering (EJGE), Vol. 22 (Bund. 14):5645-5660, 2017.*
- [11] M.Y. Fattah, N.M. Salim and I.M. Mohsin, Behavior of Single Pile in Unsaturated Clayey Soils, *Eng. & Tech. Journal, Vol. 32 Part (A), No. 3:763-787, March 2014.*
- [12] S.H. Chung and S.R. Yang, Numerical Analysis of Small Scale Model Pile in Unsaturated Clayey Soil, *Int J Civ Eng Vol 15:877–886, September 2016.*
- [13] Z. Han, S.K. Vanapalli and Z.N. Kutlu, Modeling Behavior of Friction Pile in Compacted Glacial Till, *International Journal of Geomechanics, pp.1-12, 3 March 2016.*
- [14] R.R. Al-Omari, M.Y. Fattah, and A.M. Kallawi, Laboratory Study on Load Carrying Capacity of Pile Group in Unsaturated Clay, *Arabian Journal for Science and Engineering, Vol 44(No. 5):4613–4627, July 2018.*
- [15] M.R. Mahmood, S.F.A. Al-Wakel, and A.A. Hani, Experimental and Numerical Analysis of Piled Raft Foundation Embedded with in Partially Saturated Soil, *Engineering and Technology Journal, Vol 35 Part A (No. 2):97–105, January 2017.*
- [16] D. Carvalho and A.P.J. Rocha, Uplift Behavior of Bored Piles in Tropical Unsaturated Sandy Soil, *Proceedings of The 18th International Conference on Soil Mechanics and Geotechnical Engineering, pp. 2707-2710, Paris, Perancis, 2013.*

- [17] S.K. Vanapalli and Z.N. Taylan, Design of Single Piles Using the Mechanics of Unsaturated Soils, *International Journal of Geomate, Vol.2 (No.1):197–204, March 2012.*
- [18] M.J. Tomlinson, *Pile Design and Construction Practice*, (Taylor & Francis Group E-library, 2004).
- [19] K.E. Gaaver, Uplift Capacity of Single Piles and Pile Groups Embedded in Cohesionless Soil, *Alexandria Engineering Journal, Vol. 52:365-372, 6 Januari 2013.*
- [20] H. Pujiastuti, *Perilaku Fondasi Tiang Akibat Pembebanan Pada Tanah Jenuh Sebagian (Unsaturated Soil)*, Disertasi, Departemen Teknik Sipil dan Lingkungan, Fakultas Teknik, Universitas Gadjah Mada (UGM), Yogyakarta, Indonesia, 2020.
- [21] R. Al-Omari, M. Fattah, and S. Fadhil, Adhesion Factor of Piles Embedded in Unsaturated Swelling Soil, *Proceedings of the 19th International Conference on Soil Mechanics and Geotechnical Engineering, pp. 2703-2706, Seoul, September 2017.*
- [22] M.J. Tomlinson and J. Woodward, *Pile Design and Construction Practice*, (CRS Press, Taylor and Francis Group, 2015)

Authors' information

¹ Department of Civil Engineering, Faculty of Engineering, Universitas Muhammadiyah Mataram, Mataram 83115, West Nusa Tenggara, Lombok Island, Indonesia.

² Department of Civil and Environmental Engineering, Faculty of Engineering, Universitas Gadjah Mada, Yogyakarta 55281, Indonesia.

³ Center for Disaster Mitigation and Technological Innovation (GAMA-InaTEK), Universitas Gadjah Mada, Indonesia.



Heni Pujiastuti began her civil engineering education at the Faculty of Engineering, Universitas Sebelas Maret, Indonesia in 1991. In 1998, she started her master's in Geotechnics at Universitas Gadjah Mada, Indonesia and completed. She is currently pursuing her doctorate at Universitas Gadjah Mada, Indonesia. She conducted several studies, including but not limited to shear strength of unsaturated sandy clay and bearing pile capacity in unsaturated soil.

E-mail : pujiastutih@gmail.com



Ahmad Rifa'i (corresponding author) is associate professor of Geotechnical, Civil and Environmental Engineering, Universitas Gadjah Mada (UGM) Yogyakarta. He received his doctoral degree from The Swiss Federal Institute of Technology Lausanne in 2002. Since 2008, he has been doing collaborative international research on waste materials like coal ash and volcanic ash and their potential use for soil improvement and as geo-eco-friendly materials. Rifa'i also develops equipment for mapping hydraulic properties using the constant discharge method in under saturated and unsaturated soil conditions. From 2014-2016, he used the mapping to calculate the application of volcanic ash and bantak as geo-eco-friendly structures for drainage and porous paving blocks to support restoration of heritage monuments. He is also researching unsaturated slope stability. Rifa'i is researching the comprehensive design criteria of municipal solid waste embankments in Indonesia to protect against environmental hazards. These design criteria can guide landfill design that is more sustainable for the future. A holder of seven patents, Rifa'i is a member of the Indonesian Society for Geotechnical Engineer and associate editor of GEOMATE, Japan.

E-mail : ahmad.rifai@ugm.ac.id



Darmawan Adi received his Ph.D from Strathclyde University, United Kingdom in 1996. He is currently working as an associate professor of Geotechnical, Civil and Environmental Engineering, Universitas Gadjah Mada (UGM) Yogyakarta. For the past decade he has been conducting research on investigation study of field and basic design of Jatigede hydroelectric power plant (110 MW) and effect of groundwater level changes on the parameters of clay strength. Moreover, he is a member of the Indonesian Society for Geotechnical Engineer (HATTI). Email : agusdadi@ugm.ac.id



Teuku Faisal Fathani received his Ph.D from Tokyo University of Agriculture and Technology of Japan in 2005. He is currently a professor in Civil and Environmental Engineering, Universitas Gadjah Mada (UGM) Yogyakarta. He has five patents related to multi-modal sediment disaster warning devices. He is certified as an adjunct professor of UNESCO Chair on Geoenvironmental Disaster Reduction 2018-2020. At present, he serves as the Director of Center for Disaster Mitigation and Technological Innovation (Gama-InaTEK) UGM; Vice President of International Consortium on Geo-Disaster Reduction (ICGdR); and Director of Master Program in Disaster Management (MMB), Graduate School UGM. Email : tfathani@ugm.ac.id